

Grasp Control: Theory and Experiments

Robert Platt, Roderic A. Grupen, Andrew H. Fagg

Abstract—A key problem in robot grasping is that of positioning the manipulator contacts so that an object can be grasped. In unstructured environments, contact positions are typically planned based on visual measurements that are used to reconstruct object geometry. However, because it is difficult to use vision to measure object geometry precisely in common grasp scenarios, it is useful to employ additional techniques to adjust or refine the grasp. In particular, grasp control techniques can be used to improve a grasp by adjusting the contact positions using haptic or force feedback after making initial contact with the object. This paper proposes null space grasp control, an approach that combines multiple grasp objectives to improve the grasp. Exact and approximate versions of the control law are presented. All approaches are theoretically demonstrated to converge to force closure configurations for arbitrary convex objects when grasping with a limited number of contacts. In addition, robot grasping experiments are reported that show grasp control to be practical.

I. INTRODUCTION

A key problem in robot grasping is that of positioning the contacts so that the necessary grasping forces can be applied. At each contact, the forces that can be applied depend on the local surface characteristics, including object surface normal and curvature. In unstructured environments, visual occlusions and sensor error make it difficult for a robot to measure the exact surface geometry of an object to be grasped before making contact. Therefore, the contacts must be placed on the object surface based on predictions that may be inaccurate. These predictions must ultimately be verified by force feedback when the robot actually makes contact.

When the predictions are wrong, it is advantageous to be able to adjust the manipulator configuration based on the sensed contact forces. Few approaches currently exist for accomplishing this step. After the contacts are placed on the object, how does the robot determine whether the grasp is good enough? When it is not, what mechanism can be used to displace the contacts toward better grasp locations? These two questions are the focus of the current paper. We describe key features of a non-linear control strategy that synthesizes a grasp by using contact force information to adjust contact locations. The approach is demonstrated to converge to quality grasps for a large class of objects when grasping with a limited number of contacts. Empirical results are presented that apply the approach to robot grasping of several unmodelled objects.

This paper builds upon force residual and moment residual controllers first proposed by Coelho and Grupen [1]. Coelho proved a convergence result for regular convex prismatic objects when the two controllers executed in a particular sequence and showed experimental results on a robot manipulator [2]. The current paper extends this work. First, we link the grasp controller to *unit frictionless equilibrium*, a special case of a force closure grasp. Second, we propose

the null space approach to grasp control where force and moment residual controllers execute simultaneously. Exact and approximate versions of the control law are proposed that use greater or lesser amounts of sensory feedback to converge more or less slowly. Finally, experiments are presented that demonstrate the approach to be a practical and valuable means of using force feedback to validate and improve robot grasps.

II. RELATED WORK

It is well known in the robot assembly literature that compliance in the end-effector can make insertion and assembly tasks easier [3]. When the correct admittance is used, a locally-attractive well is formed around the final configuration in the neighborhood of the insertion point. This compliance can be realized by a linear feedback controller that adjusts contact positions based on contact loads. Although end-effector admittance is not usually used to synthesize grasps, it is possible to imagine that a locally attractive control law exists that can accomplish exactly this. This is the direction of the current work. We use a non-linear feedback *grasp* control law to synthesize robot grasps using local contact information. Essentially, the robot uses haptic feedback to “feel” its way into a quality grasp configuration.

The fact that manipulator compliance can assist grasp synthesis has been demonstrated by several researchers. In these approaches, the robot selects either a pre-planned grasp or a blind “capture” and compliantly closes multiple fingers around the object. Recently, Dollar and Howe have designed a mechanically-compliant manipulator for this purpose [4]. There are several other examples of using active manipulator compliance to improve a grasp [5]. Indeed, compliance is not strictly necessary at all as several researchers have implemented robot “grab” strategies that simply close non-compliant fingers around an object [6], [7].

Relying on manipulator compliance to synthesize grasps clearly has its limit. Son, Howe, and Hagar combine visual and tactile “control primitives” to grasp a rod using a two-fingered gripper [8]. First, a tactile primitive makes contact with the object. Then, tactile sensors determine the relative gripper-object orientation and reorient the gripper so that it is better aligned with the object. Yoshimi and Allen take a completely vision-based approach and define two closed-loop visual controllers that can be combined to grasp an object [9]. The first visual servo moves the hand to the object. The second controller implements a vision-based “guarded-move.” Other examples of this type of approach are the reactive grasping algorithms proposed by Teichmann and Mishra [10]. These algorithms calculate contact displacements that provably reach a three-finger grasp in the plane. Similarly, Mirtich and Canny propose an iterative algorithm for finding quality grasps for two and three contacts in space [11].

In contrast to the above reactive and control-based approaches, a number of methods exist for planning grasp configurations given complete geometric information regarding the object. One type of approach identifies geometrical conditions among the contacts that imply a good grasp. Given these conditions, a CAD model of the object can be searched until a grasp is found. For example, Nguyen proposes several stability conditions that are searched for polygonal objects [12]. Favrejon and Ponce search the boundaries of smooth objects for antipodal configurations [13]. Sudsang and Ponce propose conditions associated with three classes of four-fingered grasps: the concurrent grasp, the pencil grasp, and the regulus grasp. Linear programming is used to find the contact configuration that satisfies the relevant condition [14]. A more complete survey of the field can be found in [15].

III. GRASP OBJECTIVE FUNCTIONS AND FORCE CLOSURE

The key idea of grasp control is to displace the contacts from an initial configuration on the object surface into a grasp configuration by using haptic or force feedback. The grasp controller reaches grasp configurations by following the gradients of two objective functions: the unit frictionless force residual and the unit frictionless moment residual. These two objective functions lead the system into *unit frictionless equilibrium* configurations. This section introduces the notion of unit frictionless equilibrium as well as the two objective functions and relates them to force closure, a common quantitative measure of a grasp.

A. Grasp Objective Functions

For the purposes of the following development, it is useful to introduce the notion of *wrench*. A wrench, $\mathbf{w} = (\mathbf{f}^T, \mathbf{m}^T)^T$, is a screw that represents a combined force, \mathbf{f} , and moment, \mathbf{m} . A system of contacts is in *equilibrium* when it is possible to apply a zero net wrench to the object while applying a strictly positive contact force with at least one of the contacts [16]. In other words, let $\hat{\mathbf{w}}_1, \dots, \hat{\mathbf{w}}_k$ be unit wrenches in the directions along which k contacts apply wrenches (the primitive contact wrenches). For a system of contacts to be in equilibrium, a set of non-negative contact force magnitudes, $\lambda_1, \dots, \lambda_k$, must exist such that

$$\sum_{i=1}^k \lambda_i \hat{\mathbf{w}}_i = \mathbf{0},$$

and $\lambda_i > 0$ for at least one contact [16].

Unit frictionless equilibrium is defined as the special case of equilibrium when all contacts apply unit forces normal to the object surface:

Definition 1: A system of k contacts is in unit frictionless equilibrium when

$$\sum_{i=1}^k \hat{\mathbf{w}}_i = \mathbf{0}.$$

When a two-contact system is in unit frictionless equilibrium, the contacts are in an anti-podal configuration (parallel and intersecting contact normals). When a three-contact system is in unit frictionless equilibrium, the contact normals lie in a plane and intersect at a single point.

Note that a system of contacts is in unit frictionless equilibrium when $\sum_{i=1}^k \hat{\mathbf{n}}_i = \mathbf{0}$ and $\sum_{i=1}^k \mathbf{r}_i \times \hat{\mathbf{n}}_i = \mathbf{0}$, where $\hat{\mathbf{n}}_i$ and \mathbf{r}_i are the unit object surface normal and the position of the i^{th} contact, respectively. Grasp control reaches unit frictionless equilibrium by defining error functions based on the above two conditions. The squared unit frictionless force residual is defined to be:

$$\epsilon_f = \frac{1}{2} \mathbf{f}^T \mathbf{f}, \quad \mathbf{f} = \sum_{i=1}^k \hat{\mathbf{n}}_i. \quad (1)$$

When the unit frictionless force residual is zero, then all of the unit normals are balanced. Such a configuration will be known as unit frictionless force equilibrium. The squared unit frictionless moment residual is defined to be:

$$\epsilon_m = \frac{1}{2} \mathbf{m}^T \mathbf{m}, \quad \mathbf{m} = \sum_{i=1}^k \mathbf{r}_i \times \hat{\mathbf{n}}_i. \quad (2)$$

It is henceforth assumed that \mathbf{m} is calculated with respect to the centroid of the contacts. When the unit frictionless moment residual is zero, then the system is in unit frictionless moment equilibrium.

B. Relationship to Force Closure

Force closure is a quantitative definition of “grasp” [16]. A force closure grasp configuration can resist arbitrary perturbation loads applied to an object (from gravity or other sources) by applying appropriate combinations of contact wrenches. Unit frictionless equilibrium is a special case of force closure for any non-zero coefficient of coulomb friction. This was demonstrated for three contacts by Ponce [14]:

Lemma 1 (Ponce): In the presence of friction (point contacts with friction), a sufficient condition for three-dimensional, d -finger force closure with $d \geq 3$ is non-marginal equilibrium.

A contact configuration is in *non-marginal equilibrium* when it is in equilibrium and all contact wrenches are *strictly* within (not on the edge of) their respective friction cones. Since unit frictionless equilibrium grasps apply forces only along the surface normals (at the center of the associated friction cone), these grasps must therefore be force closure when the contacts are able to apply positive tangential frictional forces.

The result for three contacts can be extended to two contacts if it is assumed that the contacts are able to apply frictional torsional loads about the contact normals (this is typically known as the “soft contact” assumption [16]).

Lemma 2: When at least one contact can apply frictional torsional loads about the contact normal as well as tangential frictional forces, then a sufficient condition for three-dimensional 2-finger force closure is non-marginal equilibrium.

Lemma 2 is proven in the Appendix.

IV. THE FORCE AND MOMENT RESIDUAL CONTROLLERS

Grasp control synthesizes grasps by displacing contacts over the object surface based on haptic or force sensor information. For this approach to work, sensors must be co-located with the manipulator contacts such that the local object surface characteristics (surface normal) near each contact can be measured. (Section VII summarizes the hardware required for such a configuration.) The grasp controller may begin execution when the contacts are near or in contact with the object. Presumably, the manipulator is initially placed in what is assumed to be a good grasp configuration using visual information or prior information; however, as this paper shows, the convergence of the null space grasp controller can be assured from any initial configuration. Using the sensor information and manipulator kinematics, the null space grasp control law calculates desired contact displacements that must be realized by an appropriate contact displacement mechanism. This control law descends the gradients of two control laws, the force and moment residual control laws, simultaneously. This section introduces these two control laws.

A. Force Residual Controller

Assume that the manipulator is initially in contact with a convex, second-order continuous, three-dimensional object. The force residual controller follows the negative gradient of a unit-curvature approximation of the unit frictionless force residual (Equation 1). Let the surface of the object be parameterized by orthogonal parameter curves, u and v . Let $\mathbf{r}_i(u, v)$ describe the three-dimensional Cartesian position of the i^{th} contact as a function of the parameter curves. All contact positions are measured with respect to a frame located at the multi-contact centroid. $\nabla_u \mathbf{r}_i$ and $\nabla_v \mathbf{r}_i$ denote $\frac{\partial \mathbf{r}_i}{\partial u_i}$ and $\frac{\partial \mathbf{r}_i}{\partial v_i}$, the tangents to the u and v parameter curves at contact i . Define the sense of the curves such that $(\nabla_u \mathbf{r}_i, \nabla_v \mathbf{r}_i, \hat{\mathbf{n}}_i)$ forms a right-hand orthonormal coordinate frame at each contact.

The gradient of the squared unit frictionless force residual (Equation 1) with respect to these surface coordinates is:

$$\frac{\partial \epsilon_f}{\partial \mathbf{u}} = \mathbf{f}^T J_f,$$

where $\mathbf{u} = (\mathbf{u}_1, \dots, \mathbf{u}_k)$ is a vector describing the surface coordinates of k contacts, $\mathbf{f} = \sum_{i=1}^k \hat{\mathbf{n}}_i$ is the unit frictionless force residual (Equation 1), and $J_f = \frac{\partial \mathbf{f}}{\partial \mathbf{u}}$ is the unit frictionless force residual Jacobian.

J_f may be decomposed into k partial derivatives:

$$J_{fr} = \left(\frac{\partial \mathbf{f}}{\partial \mathbf{u}_1}, \dots, \frac{\partial \mathbf{f}}{\partial \mathbf{u}_k} \right).$$

The i^{th} partial derivative can be expressed as follows:

$$\begin{aligned} \frac{\partial \mathbf{f}}{\partial \mathbf{u}_i} &= \frac{\partial \hat{\mathbf{n}}_i}{\partial \mathbf{u}_i} \\ &= (\nabla_u \mathbf{r}_i, \nabla_v \mathbf{r}_i) K_i, \end{aligned}$$

where K_i is a 2×2 symmetric positive semi-definite matrix of surface curvatures for contact i . Therefore, the unit frictionless force residual Jacobian is a matrix of surface tangents

multiplied by a matrix of surface curvatures:

$$\begin{aligned} J_f &= (\nabla_u \mathbf{r}_1, \nabla_v \mathbf{r}_1, \dots, \nabla_u \mathbf{r}_k, \nabla_v \mathbf{r}_k) K \\ &= \hat{J}_f K. \end{aligned}$$

where K is a $2k \times 2k$ symmetric positive semi-definite block diagonal matrix comprised of K_i for each contact and \hat{J}_f is a matrix whose columns are the object surface tangents at all contacts. Since for the unit sphere, K is identity and $\hat{J}_f = J_f$, we refer to \hat{J}_f as the unit-curvature frictionless force residual Jacobian.

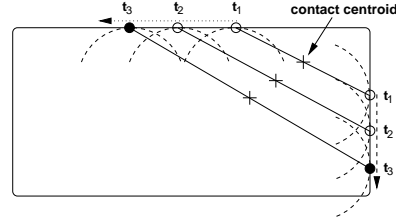


Fig. 1. The force residual controller calculates the force residual gradient by assuming that each contact normal will change as if the contact were moving on a sphere tangent to the object at the contact point. At each iteration of the controller, the gradient is recomputed using the spherical assumption.

The force residual controller follows the negative gradient of Equation 1 while assuming unit curvatures:

$$\dot{\mathbf{u}}_f = -\hat{J}_f^T \mathbf{f}. \quad (3)$$

To elucidate the effect of the force residual term of the grasp controller, consider the force residual controller executing for the planar rectangle illustrated in Figure 1. The force residual gradient assumes that the contacts are moving on surfaces with positive unit curvatures (illustrated in Figure 1 by the dotted circles). The gradient with respect to the two contact positions is illustrated by the dashed arrows pointing tangent to the object surface. The controller sends this displacement to a contact position controller. On the next cycle of the force residual controller, the contacts will have moved in the direction of the dashed arrows and the gradient will be re-evaluated as if the two dotted circles had moved with the contacts.

B. Convergence of the force residual controller

The force residual controller (Equation 3) can be shown to converge to unit frictionless force equilibrium configurations or to a class of configurations defined below as parallel opposition. First, consider the configurations where the force residual gradient (Equation 3) becomes zero. This is the case when $\mathbf{f} = 0$ or when the columns of \hat{J}_f are orthogonal to \mathbf{f} . In the latter case, all the contact surface normals must be parallel; essentially all contacts must be on the same face or parallel faces. This condition is formalized below:

Definition 2: A system of contacts is in *parallel opposition* when all contact normals are parallel, but $\mathbf{f} \neq 0$.

Clearly, Equation 3 may reach unit frictionless force equilibrium or parallel opposition. Consider the following Lyapunov

function that demonstrates that Equation 3 does not converge to any other configuration:

$$V = \frac{1}{2} \mathbf{f}^T \mathbf{f}. \quad (4)$$

The gradient of Equation 4 with respect to surface coordinates is:

$$\begin{aligned} \frac{\partial V}{\partial \mathbf{u}} &= \mathbf{f}^T \frac{\partial \mathbf{f}}{\partial \mathbf{u}} \\ &= \mathbf{f}^T \hat{J}_f K, \end{aligned}$$

where K is the symmetric positive semi-definite matrix of surface curvatures. Therefore, the gradient of \dot{V}_f along controller trajectories is:

$$\begin{aligned} \dot{V} &= \frac{\partial V}{\partial \mathbf{u}} \dot{\mathbf{u}}, \\ &= -\mathbf{f}^T \hat{J}_f K \hat{J}_f^T \mathbf{f}. \end{aligned}$$

Since K is positive semi-definite, it is clear that \dot{V}_f is negative semi-definite.

Theorem 1: Let the object be convex, second-order continuous with finite maximum curvature. Then the force residual controller (Equation 3) converges to unit frictionless force equilibrium or parallel opposition with parallel opposition being only marginally stable.

Proof: Since \dot{V} is negative semi-definite, the force residual controller (Equation 3) must be stable. It converges to configurations where \dot{V} is zero. \dot{V} is clearly zero whenever Equation 3 is zero: in unit frictionless force equilibrium or parallel opposition. In addition, it is zero when the diagonal matrix of surface curvatures, K , is zero. In this case, all contacts are on the flat faces of an object. As long as the system is not in parallel opposition, then the force residual gradient is non-zero. Each contact continues to move in a constant direction until one contact leaves its face. When this happens, the object surface curvatures are no longer zero for all contacts and the gradient of the Lyapunov function is again negative definite. While it is possible that the contact may reach another zero-curvature face, V decreases every time a contact moves from one face to another. Therefore, Equation 3 converges to unit frictionless force equilibrium or parallel opposition. Furthermore, since the Lyapunov function is not zero in parallel opposition and all neighboring non-parallel opposition configurations have smaller values of V , the fact that \dot{V} is negative semi-definite indicates that the system will move away from parallel opposition if the contacts are perturbed in the necessary way. Therefore, parallel opposition is only marginally stable. ■

Since parallel opposition is only marginally stable, we eliminate its further consideration by creating a mechanism that pushes the system out of parallel opposition when it occurs. The event of parallel opposition is easy to detect because the force residual control gradient goes to zero while the unit frictionless force residual remains non-zero. When the system is in parallel opposition, two or more contacts must be on the same face. Let S be a set of all contacts on the same

face. The control mechanism displaces each same-face contact $i \in S$ according to:

$$\dot{\mathbf{u}}_i = (\nabla_u \mathbf{r}_i, \nabla_v \mathbf{r}_i)^T \left(\mathbf{r}_i - \frac{\sum_{j \in S} \mathbf{r}_j}{|S|} \right). \quad (5)$$

It is clear that this will cause all same-face contacts to move away from each other and eventually leave the same-face configuration. Since parallel opposition is only marginally stable, the displaced contacts will not return to the prior same-face configuration. It should be noted that the above mechanism for exiting parallel opposition configurations is more important for theoretical purposes than for practical ones. Our experience with using grasp control in real robot configurations indicates that the noise and control error that is inevitable in all robot systems causes the system to exit parallel opposition configurations without special control provisions.

The requirement by Theorem 1 for the object to be second-order continuous theoretically excludes polygonal objects. Nevertheless, these objects are not excluded in practice when a manipulator with rounded contacts is used. In this case, it is possible to define a corresponding extruded object that is traced out by a point on the interior of the rounded contact. Configurations of the rounded contacts on the actual object map onto point contact configurations for the extruded object. Theorem 1 can be applied to the extruded object and, since unit frictionless equilibrium configurations for the extruded object can be shown also to be unit frictionless equilibrium on the actual object, extend to the actual object.

C. Moment Residual Controller

The moment residual controller follows the gradient of the unit frictionless moment residual while making a specific curvature assumption. The gradient of Equation 2 is:

$$\frac{\partial \epsilon_m}{\partial \mathbf{u}} = \mathbf{m}^T J_m$$

where

$$J_m = \left(\frac{\partial \mathbf{m}}{\partial u_1}, \frac{\partial \mathbf{m}}{\partial v_1}, \dots, \frac{\partial \mathbf{m}}{\partial u_k}, \frac{\partial \mathbf{m}}{\partial v_k} \right).$$

The partial derivative of the unit frictionless moment residual with respect to u_i is:

$$\frac{\partial \mathbf{m}}{\partial u_i} = \nabla_u \mathbf{r}_i \times \hat{\mathbf{n}}_i + \mathbf{r}_i \times \frac{\partial \hat{\mathbf{n}}_i}{\partial u_i},$$

Rather than incorporating surface curvature information into the moment residual gradient, the moment residual controller sets the second term to zero, effectively assuming zero surface curvature at the contacts:

$$\begin{aligned} \dot{u}_i &= \mathbf{m}^T (\nabla_u \mathbf{r}_i \times \hat{\mathbf{n}}_i) \\ &= -\mathbf{m}^T \nabla_v \mathbf{r}_i. \end{aligned}$$

Coelho refers to this simplification as the ‘‘planar assumption’’ [1]. Extending this argument to the entire moment residual control law, we have:

$$\dot{\mathbf{u}}_m = -\hat{J}_m^T \mathbf{m}, \quad (6)$$

where

$$\hat{J}_m = (-\nabla_v \mathbf{r}_1, \nabla_u \mathbf{r}_1, \dots, -\nabla_v \mathbf{r}_k, \nabla_u \mathbf{r}_k)$$

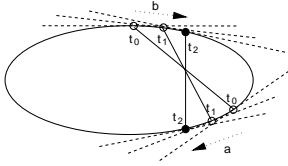


Fig. 2. The moment residual controller calculates the moment residual gradient by assuming that object geometry is a plane tangent to the object at each point of contact. At each iteration of the controller, the gradient is re-computed assuming a plane tangent to the current set of contact points.

is the zero-curvature frictionless moment residual Jacobian.

To clarify the differences between the moment residual control gradient (Equation 6) and the exact gradient, consider the planar object in Figure 2. The approximation “thinks” that the contacts will move as if the local surface were flat as illustrated by the dotted lines. Following the gradient would cause contact *a* to move to the left and contact *b* to move to the right as illustrated by the dashed arrows.

V. MULTI-OBJECTIVE GRASP CONTROL

Multi-objective grasp control concurrently evaluates the force and moment residual controllers. Null space grasp control follows the negative moment residual gradient in the null space of the change in squared force residual. This section proposes the controller and demonstrates it to converge to force closure configurations for two and three contacts.

A. Null Space Control law

In order to execute the moment residual controller concurrently with the force residual controller, a null space term can be added to the force residual controller:

$$\dot{\mathbf{u}}_n = -\hat{J}_f^T \mathbf{f} + \mathcal{N} \left(\mathbf{f}^T \hat{J}_f K \right) \dot{\mathbf{y}},$$

where $\dot{\mathbf{y}}$ is a second-priority contact displacement and K is the matrix of object surface curvatures. Since

$$\mathbf{f}^T \hat{J}_f K \mathcal{N} \left(\mathbf{f}^T \hat{J}_f K \right) \dot{\mathbf{y}} = 0,$$

regardless of the value of $\dot{\mathbf{y}}$, \dot{V}_f for this control law is still negative semi-definite and the result of Theorem 1 is unchanged. The composite null space grasp controller uses Equation 6 to select the arbitrary contact displacement, $\dot{\mathbf{y}}$. The resulting composite controller is:

$$\dot{\mathbf{u}}^* = -\hat{J}_f^T \mathbf{f} - \mathcal{N} \left(\mathbf{f}^T \hat{J}_f K \right) \hat{J}_m^T \mathbf{m}. \quad (7)$$

Theorem 1 requires Equation 7 to converge to unit frictionless force equilibrium or parallel opposition regardless of the squared unit frictionless moment residual. For two and three contact systems, it can be shown that once the system leaves a parallel opposition configuration, the force residual controller will never cause the system to return to such a configuration. Therefore, the control law introduced in Equation 5 for exiting parallel opposition configurations can be used as a pre-processing step in conjunction with Equation 7. In the sequel, we avoid further consideration of parallel opposition configurations by insisting on this pre-processing step.

B. Object surface parameterization

The result of Theorem 1 simplifies the analysis of the moment residual controller by allowing us to assume that the null space grasp controller (Equation 7) has converged to unit frictionless force equilibrium before considering the effects of the moment residual controller. Our analysis uses the following orthogonal parameterization of the object surface. This parameterization is always possible for two or three contacts in unit frictionless force equilibrium or in parallel opposition. First, let each contact, *i*, be associated with a right-handed orthogonal coordinate frame, $(\nabla_u \mathbf{r}_i, \nabla_v \mathbf{r}_i, \hat{\mathbf{n}}_i)$, where $\hat{\mathbf{n}}_i$ is the contact normal and $\nabla_u \mathbf{r}_i$ and $\nabla_v \mathbf{r}_i$ are tangents. Furthermore, let the *v* parameter curve pass through all contacts at an identical tangent such that $\nabla_v \mathbf{r}_i = \nabla_v \mathbf{r}_j = \nabla_v \mathbf{r}_k$. To construct the parameterization, let *P* be the plane in which all contact normals lie (this plane always exists for two or three contacts in unit frictionless force equilibrium or parallel opposition). Then the *v* parameter curve is defined such that the tangents are orthogonal to *P* at the contacts and the *u* parameter curve is defined such that the tangents satisfy the right hand rule at the contacts.

C. Convergence of the two-contact null space grasp controller

To demonstrate convergence for two contacts, \mathbf{r}_1 and \mathbf{r}_2 , consider the following second-order continuous positive definite function defined over two-contact configurations where the system is in unit frictionless force equilibrium or parallel opposition:

$$\begin{aligned} W &= \frac{1}{2} (\mathbf{r}_1 - \mathbf{r}_2)^T (\mathbf{r}_1 - \mathbf{r}_2) \\ &= 2\mathbf{r}_1^T \mathbf{r}_1. \end{aligned} \quad (8)$$

It is henceforth assumed that W is defined with respect to the contact centroid. For two contacts, this assumption implies that $\mathbf{r}_1 = -\mathbf{r}_2$.

W can be used to demonstrate that the composite null space grasp controller converges to unit frictionless moment equilibrium for two contacts.

Theorem 2: Let the object be convex, second-order continuous with finite maximum curvature. For two contacts, the null space grasp controller converges to unit frictionless moment equilibrium.

Proof:

The gradient of W along the trajectories of the composite null space controller is:

$$\dot{W} = -\frac{\partial W}{\partial \mathbf{u}} \left(\hat{J}_f^T \mathbf{f} + \mathcal{N} \left(\mathbf{f}^T \hat{J}_f K \right) \hat{J}_m^T \mathbf{m} \right).$$

When the system is in unit frictionless force equilibrium or parallel opposition, we have that $\hat{J}_f^T \mathbf{f} = 0$ (note that $\mathcal{N}(0)$ is the identity matrix) and:

$$\dot{W} = -\frac{\partial W}{\partial \mathbf{u}} \hat{J}_m^T \mathbf{m}.$$

Theorem 1 requires the composite null space grasp controller to converge to unit frictionless force equilibrium or

parallel opposition. However, note that, for two contacts, parallel opposition occurs when V is at a maximum (both contacts have identical surface normals). Therefore, since \dot{V} has already been shown to be negative semi-definite, the system cannot return to a parallel opposition configuration once Equation 5 has caused the system to leave such a configuration. As a result, the system must converge to unit frictionless force equilibrium.

The following facts may be verified for two contacts:

- 1) unit frictionless force equilibrium implies that $\hat{\mathbf{n}}_1 = -\hat{\mathbf{n}}_2$,
- 2) due to the required object surface parameterization, $\nabla_v \mathbf{r}_1 = \nabla_v \mathbf{r}_2$, and
- 3) the above implies that $\nabla_u \mathbf{r}_1 = -\nabla_u \mathbf{r}_2$ since $(\nabla_u \mathbf{r}_i, \nabla_v \mathbf{r}_i, \hat{\mathbf{n}}_i)$ forms a right-handed coordinate frame.

Using these facts to simplify the expression for \dot{W} , we have that:

$$\begin{aligned} \hat{J}_f^T \mathbf{m} &= \begin{bmatrix} -2(\hat{\mathbf{n}}_1 \times \nabla_v \mathbf{r}_1)^T \\ 2(\hat{\mathbf{n}}_1 \times \nabla_u \mathbf{r}_1)^T \\ -2(\hat{\mathbf{n}}_1 \times \nabla_v \mathbf{r}_1)^T \\ -2(\hat{\mathbf{n}}_1 \times \nabla_u \mathbf{r}_1)^T \end{bmatrix} \mathbf{r}_1 \\ &= 2 \begin{pmatrix} \nabla_u \mathbf{r}_1^T \\ \nabla_v \mathbf{r}_1^T \\ \nabla_u \mathbf{r}_1^T \\ -\nabla_v \mathbf{r}_1^T \end{pmatrix} \mathbf{r}_1, \end{aligned}$$

and

$$\begin{aligned} \dot{W} &= -\frac{\partial W}{\partial \mathbf{u}} \hat{J}_m^T \mathbf{m} \\ &= -\left[2 \begin{pmatrix} \nabla_u \mathbf{r}_1^T \\ \nabla_v \mathbf{r}_1^T \\ \nabla_u \mathbf{r}_1^T \\ -\nabla_v \mathbf{r}_1^T \end{pmatrix} \mathbf{r}_1 \right]^T 2 \begin{pmatrix} \nabla_u \mathbf{r}_1^T \\ \nabla_v \mathbf{r}_1^T \\ \nabla_u \mathbf{r}_1^T \\ -\nabla_v \mathbf{r}_1^T \end{pmatrix} \mathbf{r}_1 \quad (9) \\ &\leq 0. \end{aligned}$$

Since W is positive definite second order continuous and \dot{W} is negative semi-definite, the controller must converge to a configuration where $\dot{W} = 0$. If $\dot{W} = 0$, then $2\mathbf{r}_1^T \nabla_u \mathbf{r}_1 = 0$ and $2\mathbf{r}_1^T \nabla_v \mathbf{r}_1 = 0$. Therefore, $2(\mathbf{r}_1 \times \hat{\mathbf{n}}_1) = \mathbf{m} = 0$ and the system is in unit frictionless moment equilibrium. ■

D. Convergence of the three-contact null space grasp controller

A similar argument can be used to show that the composite grasp controller converges to unit frictionless moment equilibrium for three contacts. Due to space limitations, this case is not considered in the current paper.

E. Convergence to Force Closure

The preceding analysis has demonstrated that, for a large class of objects grasped with two contacts (the same can be demonstrated for three contacts), the null space grasp controller always converges to unit frictionless force equilibrium while simultaneously achieving unit frictionless moment equilibrium (Theorems 1 and 2). Lemmas 1 and 2 may be used to show that this is a sufficient condition for force closure.

Theorem 3: Let the object be convex, second-order continuous with finite maximum curvature. Then, for two contacts, the null space grasp controller (Equation 7) converges to a force closure configuration.

Proof: Theorems 1 and 2 establish that the null space grasp controller converges to unit frictionless equilibrium for two contacts. Therefore, the results of Lemmas 1 and 2 allow us to conclude force closure. ■

Note that the convergence proof for the three-contact null space grasp controller that was omitted in this paper can be used to extend Theorem 3 to the three-contact case.

VI. SWITCHING GRASP CONTROL

The null space grasp controller (Equation 7) requires knowledge of the object surface curvature, K , in order to calculate the null space projection matrix, $\mathcal{N}(\mathbf{f}^T \hat{J}_f K)$. Although sensing the object surface normal is practical using contact load cells, sensing local curvature is more difficult. One approach is to estimate curvature by sensing multiple contact normals in a neighborhood.

When curvature information cannot be measured directly, the behavior of the null space controller may be approximated by switching between the force residual controller when the system is not in unit frictionless force equilibrium ($\mathbf{f} \neq \beta$) and the moment residual controller when it is ($\mathbf{f} = 0$). We explore two related ways of accomplishing this. First, we propose a switching controller that executes the force residual controller when the unit frictionless force residual is above a specified threshold and executes the moment residual controller otherwise. Second, we propose a null space controller that approximates the projection matrix used in Equation 7 by $\mathcal{N}(\hat{J}_f)$. Both of these controllers overcome the lack of curvature information by following the full moment residual gradient only when the system reaches unit frictionless force equilibrium. Only the switching controller is demonstrated to converge to unit frictionless equilibrium. However, in Section VII, we present empirical evidence that the $\mathcal{N}(\hat{J}_f)$ also works well in practice.

A. Object surface parameterization

This section uses the same object surface parameterization that was used to demonstrate convergence of the null space grasp controller (Section V-B).

B. Force and moment residual controllers

The analysis is facilitated by writing the force and moment residual control gradients as follows. For two contacts, the moment residual gradient is:

$$\begin{aligned} \dot{\mathbf{u}}_m &= -\hat{J}_m^T \mathbf{m} \\ &= -\begin{pmatrix} -\nabla_v \mathbf{r}_1^T \\ \nabla_u \mathbf{r}_1^T \\ -\nabla_v \mathbf{r}_2^T \\ \nabla_u \mathbf{r}_2^T \end{pmatrix} (\mathbf{r}_1 \times \hat{\mathbf{n}}_1 + \mathbf{r}_2 \times \hat{\mathbf{n}}_2). \end{aligned}$$

Setting $\mathbf{r}_1 = -\mathbf{r}_2$ (assuming that these quantities are calculated with respect to an origin at the contact centroid), the

gradient becomes:

$$\dot{\mathbf{u}}_m = - \begin{pmatrix} \mathbf{r}_1^T (\nabla_u \mathbf{r}_1 - \nabla_u \mathbf{r}_2) \\ \mathbf{r}_1^T (\nabla_v \mathbf{r}_1 - \hat{\mathbf{n}}_2 \times \nabla_u \mathbf{r}_1) \\ \mathbf{r}_1^T (\nabla_u \mathbf{r}_1 - \nabla_u \mathbf{r}_2) \\ -\mathbf{r}_1^T (\nabla_v \mathbf{r}_1 - \hat{\mathbf{n}}_1 \times \nabla_u \mathbf{r}_2) \end{pmatrix}.$$

The notation in this equation and others to follow is simplified with the following substitutions:

$$p = \mathbf{r}_1^T \nabla_u \mathbf{r}_1, \quad (10)$$

$$q = \mathbf{r}_1^T \nabla_u \mathbf{r}_2, \quad (11)$$

$$s = \mathbf{r}_1^T \nabla_v \mathbf{r}_1, \quad (12)$$

$$a = \mathbf{r}_1^T (\hat{\mathbf{n}}_2 \times \nabla_u \mathbf{r}_1), \quad (13)$$

$$b = \mathbf{r}_1^T (\hat{\mathbf{n}}_1 \times \nabla_u \mathbf{r}_2). \quad (14)$$

Then, the expression for $\dot{\mathbf{u}}_m$ is:

$$\dot{\mathbf{u}}_m = - \begin{pmatrix} p - q \\ s - a \\ p - q \\ b - s \end{pmatrix}. \quad (15)$$

The force residual gradient for two contacts is:

$$\begin{aligned} \dot{\mathbf{u}}_f &= - \begin{pmatrix} \nabla_u \mathbf{r}_1^T \\ \nabla_v \mathbf{r}_1^T \\ \nabla_u \mathbf{r}_2^T \\ \nabla_v \mathbf{r}_2^T \end{pmatrix} \mathbf{f} \\ &= - \begin{pmatrix} \nabla_u \mathbf{r}_1^T \hat{\mathbf{n}}_2 \\ 0 \\ \nabla_u \mathbf{r}_2^T \hat{\mathbf{n}}_1 \\ 0 \end{pmatrix}. \end{aligned} \quad (16)$$

If an additional substitution,

$$\alpha = \nabla_u \mathbf{r}_1^T \hat{\mathbf{n}}_2 = -\nabla_u \mathbf{r}_2^T \hat{\mathbf{n}}_1, \quad (17)$$

is allowed (see Lemma 3 in the Appendix for the demonstration that $\nabla_u \mathbf{r}_1^T \hat{\mathbf{n}}_2 = -\nabla_u \mathbf{r}_2^T \hat{\mathbf{n}}_1$), then this gradient is written more compactly as:

$$\dot{\mathbf{u}}_f = - \begin{pmatrix} \alpha \\ 0 \\ -\alpha \\ 0 \end{pmatrix}.$$

C. Switched grasp controller

The switching grasp controller switches between executing the force residual controller when $\|\mathbf{f}\| > \beta$ and executing the moment residual controller when $\|\mathbf{f}\| \leq \beta$. This is accomplished using an indicator variable:

$$N_a = \begin{cases} 1 & \text{if } \|\mathbf{f}\| > \beta \\ 0 & \text{otherwise} \end{cases}$$

The resulting controller is:

$$\dot{\mathbf{u}}_a = \dot{\mathbf{u}}_f + N_a \dot{\mathbf{u}}_m. \quad (18)$$

As with the null space controller, we require Equation 5 to execute as a pre-processing step to lead the system out of parallel opposition configurations.

To demonstrate that the switching controller converges to unit frictionless equilibrium, consider its behavior with respect to V , the force residual Lyapunov function (Equation 4), and W , the two-contact positive definite function (Equation 8).

Performing a similar calculation to that in Equation 16, the derivative of V with respect to surface coordinates for two contacts is:

$$\frac{\partial V}{\partial \mathbf{u}} = \begin{pmatrix} \alpha \\ 0 \\ -\alpha \\ 0 \end{pmatrix} K.$$

The derivative of W with respect to surface coordinates for two contacts is:

$$\frac{\partial W}{\partial \mathbf{u}} = 2 \begin{pmatrix} \mathbf{r}_1^T \nabla_u \mathbf{r}_1 \\ \mathbf{r}_1^T \nabla_v \mathbf{r}_1 \\ -\mathbf{r}_1^T \nabla_u \mathbf{r}_1 \\ -\mathbf{r}_1^T \nabla_v \mathbf{r}_1 \end{pmatrix} = 2 \begin{pmatrix} p \\ s \\ -q \\ -s \end{pmatrix}. \quad (19)$$

In order to establish convergence, it will be useful to evaluate the gradients of V and W for the two cases, $\|\mathbf{f}\| \leq \beta$ and $\|\mathbf{f}\| > \beta$. First, consider the case where $\|\mathbf{f}\| > \beta$ and $N_a = 0$. Then $\dot{\mathbf{u}}_a = \dot{\mathbf{u}}_f$ and:

$$\begin{aligned} \dot{V}_{\|\mathbf{f}\| > \beta} &= -\frac{\partial V}{\partial \mathbf{u}} \dot{\mathbf{u}}_f \\ &= \begin{pmatrix} \alpha \\ 0 \\ -\alpha \\ 0 \end{pmatrix}^T K \begin{pmatrix} \alpha \\ 0 \\ -\alpha \\ 0 \end{pmatrix} \\ &= -(\kappa_1 + \kappa_4) \alpha^2. \end{aligned} \quad (20)$$

where κ_1 and κ_4 are elements of the matrix of object surface curvatures, K . The gradient of W when $\|\mathbf{f}\| > \beta$ is:

$$\begin{aligned} \dot{W}_{\|\mathbf{f}\| > \beta} &= -2 \begin{pmatrix} p \\ s \\ -q \\ -s \end{pmatrix}^T \begin{pmatrix} \alpha \\ 0 \\ -\alpha \\ 0 \end{pmatrix} \\ &= -2(p + q)\alpha. \end{aligned} \quad (21)$$

When $\|\mathbf{f}\| \leq \beta$, then $N_a = 1$ and $\dot{\mathbf{u}}_a = \dot{\mathbf{u}}_f + \dot{\mathbf{u}}_m$. In this situation, we have:

$$\begin{aligned} \dot{V}_{\|\mathbf{f}\| \leq \beta} &= -\frac{\partial V}{\partial \mathbf{u}} (\dot{\mathbf{u}}_f + \dot{\mathbf{u}}_m) \\ &= - \begin{pmatrix} \alpha \\ 0 \\ -\alpha \\ 0 \end{pmatrix} K \begin{pmatrix} p - q + \alpha \\ s - a \\ p - q - \alpha \\ b - s \end{pmatrix} \\ &= -(\kappa_1 + \kappa_4) \alpha^2 \\ &\quad -\alpha(\kappa_1 - \kappa_4)(p - q) \\ &\quad -\alpha\kappa_2(s - a) - \alpha\kappa_5(s - b), \end{aligned} \quad (22)$$

where κ_2 and κ_5 are elements of the curvature matrix, K . The

gradient of W when $\|\mathbf{f}\| \leq \beta$ is:

$$\begin{aligned} \dot{W}_{\|\mathbf{f}\| \leq \beta} &= -\frac{\partial W}{\partial \mathbf{u}}(\dot{\mathbf{u}}_f + \dot{\mathbf{u}}_m) \\ &= -2 \begin{pmatrix} p \\ s \\ -q \\ -s \end{pmatrix}^T \begin{pmatrix} p - q + \alpha \\ s - a \\ p - q - \alpha \\ b - s \end{pmatrix} \\ &= -2(p - q)^2 - 2s(s - a) - 2s(s - b) \\ &\quad - 2(p + q)\alpha. \end{aligned} \quad (23)$$

The following theorem establishes convergence for the switching controller.

Theorem 4: Let the object be convex, second-order continuous, with finite maximum curvature. Then the switching grasp controller (Equation 18) approaches unit frictionless equilibrium as the controller's β parameter goes to zero.

Proof:

If both contacts are not on the same face, then $\dot{V}_{\|\mathbf{f}\| > \beta}$ (Equation 20) is negative definite. Therefore, $\|\mathbf{f}\|$ decreases until $\|\mathbf{f}\| \leq \beta$. When this happens, notice that $\dot{V}_{\|\mathbf{f}\| \leq \beta}$ (Equation 22) may be positive or negative. We show that in either case, the system converges to unit frictionless equilibrium.

First, if $\dot{V}_{\|\mathbf{f}\| \leq \beta}$ is negative, then \mathbf{f} converges to zero and since $\|\alpha\| \leq \|\mathbf{f}\|$ (Lemma 4), α also converges to zero. Substituting $\alpha = 0$ into Equation 23, we have that $\dot{W}_{\|\mathbf{f}\| \leq \beta}$ is negative semi-definite because sa and sb are negative. Since W is smooth and positive definite, the controller converges to a configuration where $\dot{W}_{\|\mathbf{f}\| \leq \beta} = 0$. Note that $p = -q$ when $\mathbf{f} = 0$. Therefore, $\dot{W}_{\|\mathbf{f}\| \leq \beta} = 0$ implies that p , q , and s are zero and that \mathbf{r}_1 is perpendicular to the object surface at the contacts. Therefore, we have converged to a configuration where both \mathbf{f} and \mathbf{m} are zero.

Second, if $\dot{V}_{\|\mathbf{f}\| \leq \beta}$ is positive, then the controller oscillates between configurations where $\|\mathbf{f}\| > \beta$ and $\|\mathbf{f}\| \leq \beta$. Since it may be that $\|\dot{V}_{\|\mathbf{f}\| \leq \beta}\| \neq \|\dot{V}_{\|\mathbf{f}\| > \beta}\|$, several iterations of the controller may execute in one control mode for every one iteration in the other mode. Without loss of generality, assume that when $\|\mathbf{f}\| > \beta$, the controller executes γ iteration for every one iteration executed when $\|\mathbf{f}\| \leq \beta$ such that: $\dot{V}_{\|\mathbf{f}\| \leq \beta} = -\gamma \dot{V}_{\|\mathbf{f}\| > \beta}$. Solving for $1 + \gamma$ (using Equations 20 and 22), we have:

$$1 + \gamma = \frac{\Gamma}{\alpha},$$

where

$$\Gamma = -\frac{(\kappa_1 - \kappa_4)(p - q) + \kappa_2(s - a) + \kappa_5(s - b)}{\kappa_1 + \kappa_4}.$$

Assuming that the system is locally linear (valid for small step sizes), then the contact displacement caused by γ control iterations is approximately $\gamma \dot{\mathbf{u}}_a$. Therefore, the change in W when $\|\mathbf{f}\| > \beta$ is $\gamma \dot{W}_{\|\mathbf{f}\| > \beta}$ and the net change in W as the

system oscillates in a neighborhood of $\|\mathbf{f}\| = \beta$ is:

$$\begin{aligned} \dot{W} &= \gamma \dot{W}_{\|\mathbf{f}\| > \beta} + \dot{W}_{\|\mathbf{f}\| \leq \beta} \\ &= -2[(p - q)^2 + s(s - a) + s(s - b) \\ &\quad + (1 + \gamma)(p + q)\alpha] \\ &= -2[(p - q)^2 + s(s - a) + s(s - b) \\ &\quad + \Gamma(p + q)]. \end{aligned} \quad (24)$$

The magnitude of $p + q$ can be bounded by recognizing that $\hat{\mathbf{n}}_1$ and $\nabla_u \mathbf{r}_1$ are related by the same rotation matrix that relates $\hat{\mathbf{n}}_2$ and $\nabla_u \mathbf{r}_2$: $\hat{\mathbf{n}}_1 = R \nabla_u \mathbf{r}_1$ and $\hat{\mathbf{n}}_2 = R \nabla_u \mathbf{r}_2$. Therefore:

$$\begin{aligned} \|\nabla_u \mathbf{r}_1 + \nabla_u \mathbf{r}_2\| &= \|R^T \hat{\mathbf{n}}_1 + R^T \hat{\mathbf{n}}_2\| \\ &= \|\hat{\mathbf{n}}_1 + \hat{\mathbf{n}}_2\| \\ &= \|\mathbf{f}\|, \end{aligned}$$

and

$$\begin{aligned} p + q &\leq \|\mathbf{r}_1\| \|\nabla_u \mathbf{r}_1 + \nabla_u \mathbf{r}_2\| \\ &\leq \|\mathbf{r}_1\| \|\mathbf{f}\|, \end{aligned}$$

where the last inequality used Lemma 4 in the Appendix.

With the above fact in mind, it is clear that the $\Gamma(p + q)$ term in Equation 24 can be made arbitrarily small by reducing β . Since sa and sb are negative (Lemma 5), it is therefore always possible to make \dot{W} negative when $\mathbf{m} \neq 0$ by reducing β . Therefore, as β goes to zero, \mathbf{f} goes to zero, \dot{W} goes to zero, p , q , s go to zero, and therefore, \mathbf{m} goes to zero.

In conclusion, we have shown that when $\dot{V}_{\|\mathbf{f}\| \leq \beta}$ is negative or positive, the system approaches a unit frictionless equilibrium configuration as β goes to zero. ■

D. Approximate null space grasp controller

The switching controller converges to unit frictionless equilibrium more slowly than the null space controller because it does not execute the moment residual controller until reaching unit frictionless force equilibrium. The approximate null space controller projects the moment residual controller into the null space of \hat{J}_f :

$$\dot{\mathbf{u}}_j = \dot{\mathbf{u}}_f + \mathcal{N}(\hat{J}_f) \dot{\mathbf{u}}_m. \quad (25)$$

This has the effect of switching off part, but not all, of the moment residual controller when $\mathbf{f} \neq 0$. The result is that $\dot{V}_{\mathbf{f} \neq 0}$ is not necessarily negative semi-definite and it is more difficult to prove convergence. Nevertheless, Section VII demonstrates good practical results with this controller.

VII. EXPERIMENTS

The experiments evaluate the approximate null space grasp controller (Equation 25). Although the convexity assumption is not satisfied, the controller still reaches force closure configurations in most cases. All experiments were conducted using Dexter, a bimanual dexterous humanoid robot at the University of Massachusetts Amherst. Dexter consists of two whole arm manipulators (WAMs), two Barrett hands equipped with six-axis load cells at the fingertips, and a Bisight stereo camera system.

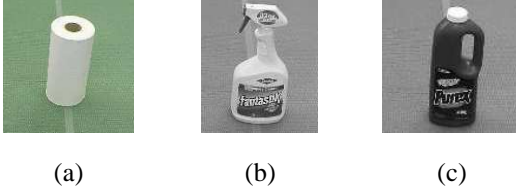


Fig. 3. Three objects for which the grasp controller was tested.

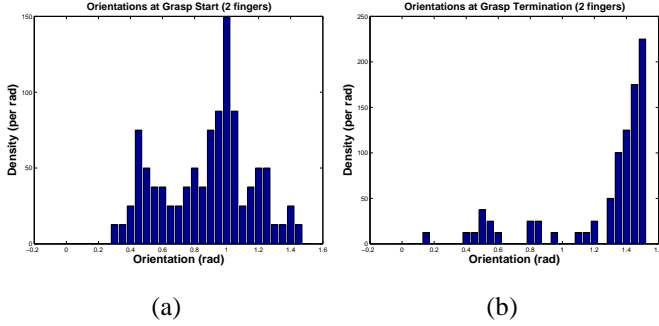


Fig. 4. Experiment 1 (towel roll, two contacts): the distribution of contact orientations before, (a), and after, (b), the grasp controller has executed. Orientation is the angle between a line that passes between the two grasp contacts and the major axis of the object (see text).

Contact displacements were realized by a hybrid force-position controller that applied a small inward force at each contact along the inward contact surface normal while displacing the contacts tangent to the surface. The contacts tracked the velocities specified by the grasp controller as closely as the manipulator kinematic constraints allowed.

A. Experiment 1: Grasping a Towel Roll Using Two Virtual Fingers

In the first experiment, the approximate null space grasp controller was used to synthesize 58 two-contact grasps of the vertical towel roll (10cm diameter and 20cm tall) shown in Figure 3(a). On each trial, the grasp controller began execution in a randomly selected configuration relative to the object and continued until controller convergence or until the human operator detected that the manipulator had collided with the environment. Two of the three fingers on the Barrett hand were grouped together as a single contact (a virtual finger) [17], [18].

Figures 4(a) and 4(b) show the density of hand orientations before and after executing the grasp controller. Hand orientation is measured by the angle between the line that connects the two virtual contacts and the towel roll major axis. The Figures show that for the vertical towel roll, the two-contact grasp controller aligned the hand orthogonal to the major axis of the cylinder on most of the grasp trials. However, on a few trials, the controller terminated near the small peak at 0.45 radians in Figure 4(b). These trials were terminated by the human operator because the Barrett hand palm collided with the object. These collisions highlight the fact that, without any provision for obstacle avoidance or

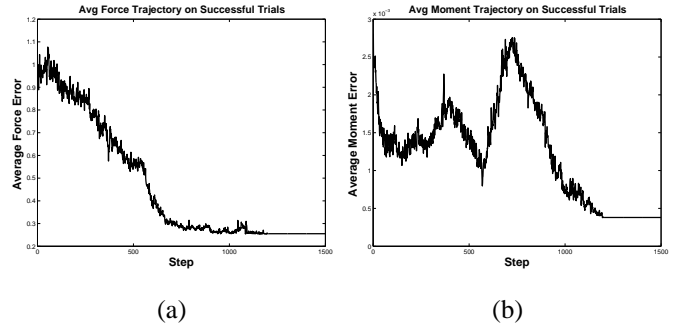


Fig. 5. Experiment 1 (towel roll, two contacts): average squared force residual, (a), and average squared moment residual, (b), for the grasp trials that terminated near the peak at $\pi/2$ in Figure 4(b).

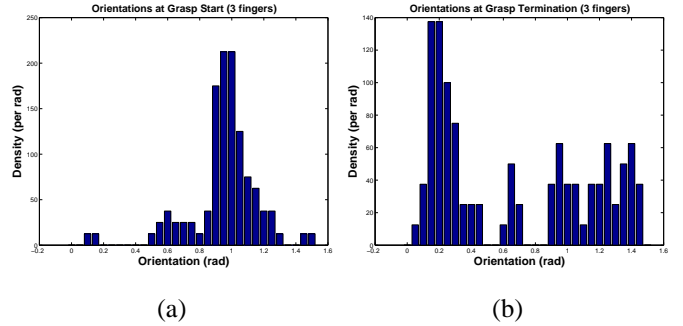


Fig. 6. Experiment 2 (towel roll, three contacts): the distribution of contact orientations before, (a), and after, (b), the three-contact grasp controller has executed. Orientation is the angle between a normal to the plane of the three grasp contacts and the major axis (see text).

configuration optimization, limitations on contact mobility may interfere with grasp controller performance. On these grasp trials, one of the grasp contacts was on the top of the cylinder while the other was on the side. As the grasp controller displaced the contacts around the object, it did not take the limited aperture of the Barrett hand into account and caused a collision.

Figure 5 illustrates the average force and moment residual error trajectories for the grasp trials that comprise the peak near $\pi/2$ in Figure 4(b). Figure 5(a) shows the average force error (squared force residual) while Figure 5(b) shows the average moment error. The horizontal axis in both figures is grasp controller step. The graphs illustrate that, on average, both force and moment errors converge to configurations with small wrench residuals in approximately 1000 steps (20 seconds, not including the time taken to tare the fingertip load cells.)

B. Experiment 2: Grasping a Towel Roll Using Three Contacts

In the second experiment, the approximate null space grasp controller was used to grasp the vertical towel roll (Figure 3(a)) using three contacts. Figures 6(a) and 6(b) show the density of hand orientations before and after grasp synthesis. In the figure, orientation is measured by the angle between the normal to the plane containing the three fingertips and the major axis of the cylinder. The results show that the grasp

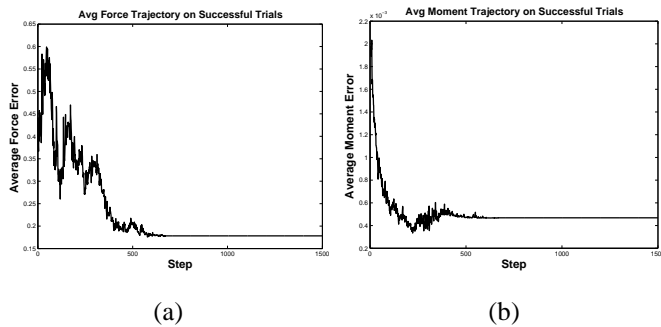


Fig. 7. Experiment 3 (squirt bottle, two contacts): average force residual, (a), and moment residual, (b).

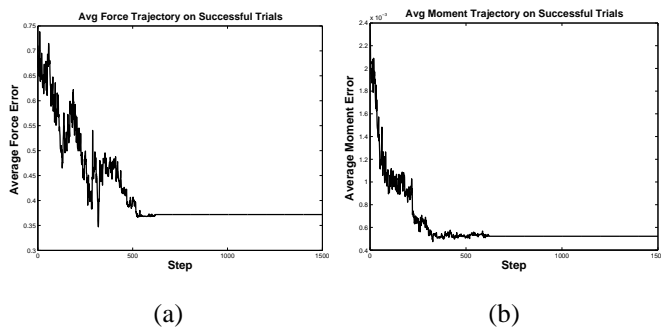


Fig. 8. Experiment 3 (detergent bottle, two contacts): average force residual, (a), and moment residual, (b).

controller displaced the contacts from a starting distribution of hand orientations near 1 radian to a peak near 0 radians (the peak near 0 corresponds to an intuitively correct top grasp where the normal of the contact plane is parallel to the cylinder major axis.)

The histogram of final palm orientations shown in Figure 6(b) shows that in several cases, the grasp controller found configurations where the hand was oriented between 0.8 and 1.6 radians. These trials were terminated by the human operator because of a collision. As in Experiment 1, these failures result from the fact that Equation 25 does not make any provision for obstacle avoidance or manipulator optimization. In these cases, the grasp controller placed one of the contacts on top of the cylinder and attempted to move the other two contacts toward the other end. While a lengthwise grasp is theoretically possible, aperture constraints prevent this grasp from working in practice.

C. Experiment 3: Grasping a Squirt Bottle and a Detergent Bottle

Experiment 3 uses the approximate null space grasp controller to synthesize grasps of the squirt bottle and detergent bottle shown in Figures 3(b) and 3(c) using two contacts. The experimental procedure was the same as that used in experiments 1 and 2. On each trial, the grasp controller started from a randomly selected configuration. 28 grasp synthesis trials were executed for the squirt bottle and 31 grasps for the detergent bottle. Whereas the grasp controller had problems with kinematic limitations of the manipulator when grasping

the cylinder, there were no such problems with the squirt and detergent bottles because, for these objects, the grasp controller tended away from grasp configurations that caused the manipulator to collide with the table. Figures 7 and 8 show that the grasp controller found low-error grasps for these objects.

VIII. CONCLUSION

Rather than planning contact positions based on prior information, grasp control uses haptically-measured feedback to synthesize grasps. An analogy can be drawn between the use of manipulator compliance in insertion tasks and grasp control in grasping tasks. In both cases, a control law using local force feedback is used to adjust what might initially be only an approximate solution. Both methods can make the fine adjustments in manipulator configuration that are extremely difficult to achieve in other ways.

This paper focuses on a theoretical understanding of multi-objective grasp control. Two approaches are proposed: null space grasp control and switched grasp control. Both control laws are shown to realize force closure grasps by executing two component control laws concurrently. The null space controller uses measurements of surface curvature to synthesize grasps by projecting one component controller into the null space of the gradient of the other. The switching controller approximates the null space composition by alternating between the two control laws. The switching controller achieves the same force closure grasps as the null space controller without requiring surface curvature measurements. Results from grasp experiments performed on a real robot corroborate the theoretical results. Our experimental work indicates that grasp control is a practical way to synthesize and improve grasps.

From a theoretical perspective, an important remaining question is whether convergence can be established for the approximate null space controller of Equation 25. Our experimental results suggest that this controller works well. However, the controller has not yet been shown to converge for all convex objects. From a broader perspective, there are many ways that force and haptic information might be used to assist robot grasping. Intuition suggests that humans rely on a sense of touch to grasp without looking at the object and to make grasping more robust. We expect that this will continue to be an important research question in the future.

APPENDIX

The following Lemma was used in Section III-B and is proven below.

Lemma 2: When the contacts can apply frictional torsional loads about the contact normal as well as tangential frictional forces, then a sufficient condition for three-dimensional two-finger force closure is non-marginal equilibrium.

Proof: Let \mathbf{f}_1 and \mathbf{f}_2 be equilibrium forces on the object. Let a_1 and a_2 be equilibrium contact moments (induced by the soft contacts) about the surface normals. Let \mathbf{r}_1 and \mathbf{r}_2 be the contact positions in a coordinate frame centered outside

the object. Let \mathbf{f} and \mathbf{m} be the components of an arbitrary wrench applied to the object. Let β be the component of \mathbf{m} orthogonal to $\mathbf{r}_1 - \mathbf{r}_2$. Let α be the other component.

Since the system is in equilibrium, we have that $\mathbf{f}_1 + \mathbf{f}_2 = 0$ and $\mathbf{r}_1 \times \mathbf{f}_1 + \mathbf{r}_2 \times \mathbf{f}_2 + a_1 + a_2 = 0$. Let $\mathbf{f}'_1 = \mathbf{f}_1 - \mathbf{f} + \mathbf{v}$, $\mathbf{f}'_2 = \mathbf{f}_2 - \mathbf{v}$, $a'_1 = a_1 - \alpha$, and $a'_2 = a_2$ where

$$\mathbf{v} = (\mathbf{x}_1 \times \mathbf{f} - \beta) \times (\mathbf{x}_1 - \mathbf{x}_2).$$

Then, we have that $\mathbf{f}'_1 + \mathbf{f}'_2 = -\mathbf{f}$ and $a'_1 + a'_2 + \mathbf{r}_1 \times \mathbf{f}'_1 + \mathbf{r}_2 \times \mathbf{f}'_2 = -\mathbf{m}$. Therefore, it is possible to resist an arbitrary wrench, \mathbf{f} and \mathbf{m} , as long as \mathbf{f}'_1 , \mathbf{f}'_2 , a'_1 , and a'_2 are within their friction cones. Following the argument in [14], for any force difference \mathbf{c} , it is possible to apply the net force, $\mathbf{f}'_1 = \gamma \mathbf{f}_1 + \mathbf{c}$ by increasing γ sufficiently. Similarly, arbitrary moments about the contact normal can be applied. ■

The following three lemmas are used in Section VI.

Lemma 3: Let $(\mathbf{u}_1, \mathbf{v}_1, \mathbf{n}_1)$ and $(\mathbf{u}_2, \mathbf{v}_2, \mathbf{n}_2)$ be two orthonormal right-handed coordinate frames such that $\mathbf{v}_1 = \mathbf{v}_2$. Then $\mathbf{n}_1^T \mathbf{u}_2 = -\mathbf{n}_2^T \mathbf{u}_1$.

Proof:

Let R be a rotation matrix that describes the relationship between the two coordinate frames:

$$(\mathbf{u}_2, \mathbf{v}_2, \mathbf{n}_2) = R(\mathbf{u}_1, \mathbf{v}_1, \mathbf{n}_1).$$

Let Φ describe a 90 degree rotation about $\mathbf{v}_1 = \mathbf{v}_2$ such that:

$$\mathbf{n}_1 = \Phi \mathbf{u}_1,$$

and

$$\mathbf{n}_2 = \Phi \mathbf{u}_2.$$

Then:

$$\begin{aligned} \mathbf{n}_1^T \mathbf{u}_2 &= \mathbf{n}_1^T R \mathbf{u}_1 \\ &= (\Phi \mathbf{u}_1)^T R \Phi^T \mathbf{n}_1 \\ &= \mathbf{u}_1^T \Phi^T R \Phi^T \mathbf{n}_1. \end{aligned}$$

Since both Φ and R rotate about $\mathbf{v}_1 = \mathbf{v}_2$, these rotation matrices commute:

$$\Phi^T R \Phi^T = R \Phi^T \Phi^T.$$

However, notice that since Φ^T rotates through 90 degrees, $\Phi^T \Phi^T$ rotates through 180 degrees, or:

$$\begin{aligned} \mathbf{n}_1^T \mathbf{u}_2 &= \mathbf{u}_1^T \Phi^T R \Phi^T \mathbf{n}_1 \\ &= \mathbf{u}_1^T R \Phi^T \Phi^T \mathbf{n}_1 \\ &= -\mathbf{u}_1^T R \mathbf{n}_1 \\ &= -\mathbf{u}_1^T \mathbf{n}_2. \end{aligned}$$

■

Lemma 4: Let $(\mathbf{u}_1, \mathbf{v}_1, \mathbf{n}_1)$ and $(\mathbf{u}_2, \mathbf{v}_2, \mathbf{n}_2)$ be two orthonormal right-handed coordinate frames such that $\mathbf{v}_1 = \mathbf{v}_2$ and $\mathbf{n}_1^T \mathbf{n}_2 \leq 0$. Then

$$\|\mathbf{n}_2^T \mathbf{u}_1\| \leq \|\mathbf{f}\| \leq \sqrt{2} \|\mathbf{n}_2^T \mathbf{u}_1\|,$$

where $\mathbf{f} = \mathbf{n}_1 + \mathbf{n}_2$.

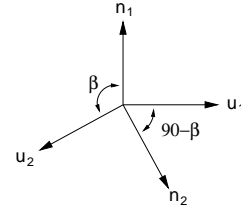


Fig. 9. Geometry of β .

Proof: Let β be the magnitude of the angle between \mathbf{n}_1 and \mathbf{n}_2 . Since $\mathbf{n}_1^T \mathbf{n}_2 \leq 0$, then β must be bounded by: $90 \leq \beta \leq 180$.

Since $\mathbf{v}_1 = \mathbf{v}_2$, then $\mathbf{n}_1, \mathbf{n}_2, \mathbf{u}_1$, and \mathbf{u}_2 lie in a plane. By the geometry of the situation, the magnitude of the angle between \mathbf{n}_2 and \mathbf{u}_1 is $\beta - 90$ (see Figure 9). Therefore:

$$\begin{aligned} \|\mathbf{n}_2^T \mathbf{u}_1\| &= \cos(\beta - 90) \\ &= \|\sin \beta\| \\ &= 2 \|\sin \frac{\beta}{2} \cos \frac{\beta}{2}\|. \end{aligned}$$

Let \mathbf{h} be the unit vector such that:

$$\mathbf{n}_1 + \mathbf{n}_2 = \|\mathbf{f}\| \mathbf{h},$$

and $\|\mathbf{f}\| = \|\mathbf{n}_1 + \mathbf{n}_2\|$. Then

$$\|\mathbf{f}\| = \|\mathbf{h}^T \mathbf{n}_1\| + \|\mathbf{h}^T \mathbf{n}_2\|.$$

Let γ be the angle between \mathbf{h} and \mathbf{n}_1 such that

$$\begin{aligned} \cos \frac{\beta}{2} &= \cos \gamma \\ &= \|\mathbf{h}^T \mathbf{n}_1\| \\ &= \|\mathbf{h}^T \mathbf{n}_2\| \\ &= \frac{\|\mathbf{f}\|}{2}. \end{aligned}$$

Since $\sin \frac{\beta}{2} \leq 1$, we have that:

$$\begin{aligned} \|\mathbf{n}_2^T \mathbf{u}_1\| &= \|2 \sin \frac{\beta}{2} \cos \frac{\beta}{2}\| \\ &\leq 2 \|\cos \frac{\beta}{2}\| \\ &\leq \|\mathbf{f}\|. \end{aligned}$$

Also, since $\beta \geq 90$ by assumption, then $\sin \frac{\beta}{2} \geq \frac{1}{\sqrt{2}}$ and we have:

$$\begin{aligned} \|\hat{\mathbf{n}}_2^T \mathbf{u}_1\| &= \|2 \sin \frac{\beta}{2} \cos \frac{\beta}{2}\| \\ &\geq \sqrt{2} \|\cos \frac{\beta}{2}\| \\ &\geq \frac{1}{\sqrt{2}} \|\mathbf{f}\|. \end{aligned}$$

Combining the above bounds on $\|\mathbf{f}\|$, we have:

$$\|\hat{\mathbf{n}}_2^T \mathbf{u}_1\| \leq \|\mathbf{f}\| \leq \sqrt{2} \|\hat{\mathbf{n}}_2^T \mathbf{u}_1\|.$$

■

Lemma 5: Let $(\mathbf{u}_1, \mathbf{v}_1, \mathbf{n}_1)$ and $(\mathbf{u}_2, \mathbf{v}_2, \mathbf{n}_2)$ be two coordinate frames such that $\mathbf{v}_1 = \mathbf{v}_2$ and $\mathbf{n}_1^T \mathbf{n}_2 \leq 0$. Let $s = \mathbf{r}^T \mathbf{v}_1$,

$a = \mathbf{r}^T(\mathbf{n}_2 \times \mathbf{u}_1)$, and $b = \mathbf{r}^T(\mathbf{n}_1 \times \mathbf{u}_2)$ for an arbitrary vector, \mathbf{r} . Then $s = 0$ implies that $a = 0$ and $b = 0$. Also, $sa \leq 0$ and $sb \leq 0$.

Proof: Since $\mathbf{v}_1 = \mathbf{v}_2$, we have that $\mathbf{u}_1, \mathbf{n}_1, \mathbf{u}_2$, and \mathbf{n}_2 are orthogonal to \mathbf{v}_1 . Therefore, $\mathbf{n}_2 \times \mathbf{u}_1 = \gamma \mathbf{v}_1$ and $\mathbf{n}_1 \times \mathbf{u}_2 = \eta \mathbf{v}_1$ where $\gamma = (\mathbf{n}_2 \times \mathbf{u}_1)^T \mathbf{v}_1$ and $\eta = (\mathbf{n}_1 \times \mathbf{u}_2)^T \mathbf{v}_1$. a and b can be rewritten: $a = \gamma s$ and $a = \eta s$. Therefore, we have that $s = 0$ implies that $a = 0$ and $b = 0$.

Note that γ and η must be negative:

$$\begin{aligned} \gamma &= (\mathbf{n}_2 \times \mathbf{u}_1)^T \mathbf{v}_1 \\ &= \mathbf{n}_2^T (\mathbf{u}_1 \times \mathbf{v}_1) \\ &= \mathbf{n}_2^T \mathbf{n}_1 \\ &\leq 0, \end{aligned}$$

and

$$\begin{aligned} \eta &= (\mathbf{n}_1 \times \mathbf{u}_2)^T \mathbf{v}_1 \\ &= \mathbf{n}_1^T (\mathbf{u}_2 \times \mathbf{v}_2) \\ &= \mathbf{n}_1^T \mathbf{n}_2 \\ &\leq 0. \end{aligned}$$

We can conclude that sa and sb are negative because:

$$\begin{aligned} sa &= \mathbf{r}^T \mathbf{v}_1 \mathbf{r}^T (\mathbf{n}_2 \times \mathbf{u}_1) \\ &= \gamma \mathbf{r}^T \mathbf{v}_1 \mathbf{v}_1^T \mathbf{r} \\ &\leq 0, \end{aligned}$$

and

$$\begin{aligned} sb &= \mathbf{r}^T \mathbf{v}_1 \mathbf{r}^T (\mathbf{n}_1 \times \mathbf{u}_2) \\ &= \eta \mathbf{r}^T \mathbf{v}_1 \mathbf{v}_1^T \mathbf{r} \\ &\leq 0. \end{aligned}$$

■

REFERENCES

- [1] J. Coelho and R. Grupen, "A control basis for learning multifingered grasps," *Journal of Robotic Systems*, 1997.
- [2] J. Coelho, "Multifingered grasping: Grasp reflexes and control context," Ph.D. dissertation, University of Massachusetts, 2001.
- [3] D. E. Whitney, "Historical perspective and state of the art in robot force control," *Int. Journal of Robotics Research*, vol. 6, no. 1, pp. 3–14, 1987.
- [4] A. Dollar and R. Howe, "A robust compliant grasping via shape deposition manufacturing," *IEEE Transactions on Mechatronics*, vol. 11, no. 2, pp. 154–161, 2006.
- [5] A. Edsinger, "Robot manipulation in human environments," Ph.D. dissertation, MIT, 2007.
- [6] D. Roy, "Semiotic schemas: a framework for grounding language in action and perception," *Artificial Intelligence*, vol. 167, no. 1-2, pp. 170–205, 2005.
- [7] T. B. Martin, R. O. Ambrose, M. A. Diftler, R. P. Jr., and M. J. Butzer, "Tactile gloves for autonomous grasping with the nasa/darpa robonaut," in *IEEE Conference on Robotics and Automation*, April 2004.
- [8] J. Son, R. Howe, J. Wang, and G. Hager, "Preliminary results on grasping with vision and touch," in *IEEE Int'l Conf. on Intelligent Robots and Systems*, vol. 3, November 1996.
- [9] B. Yoshimi and P. Allen, "Integrating real-time vision and manipulation," in *Proc. of 13th Hawaii Int'l Conf. on System Sciences*, vol. 5, January 1997, pp. 178–187.
- [10] M. Teichmann and B. Mishra, "Reactive algorithms for 2 and 3 finger grasping," in *International Symposium on Intelligent Robotic Systems*, July 1994.
- [11] B. Mirtich and J. Canny, "Easily computable optimum grasps in 2-d and 3-d," in *IEEE Int'l Conf. Robotics Automation*, 1994, pp. 739–747.

- [12] V. Nguyen, "Constructing stable grasps in 3d," in *IEEE Int'l Conf. Robotics Automation*, vol. 4, March 1987, pp. 234–239.
- [13] B. Faverjon and J. Ponce, "On computing two-finger force-closure grasps of curved 2d objects," in *IEEE Int'l Conf. Robotics Automation*, 1991.
- [14] J. Ponce, S. Sullivan, A. Sudsang, J. Boissonnat, and J. Merlet, "On computing four-finger equilibrium and force-closure grasps of polyhedral objects," *Int. J. Rob. Res.*, 1996.
- [15] A. Bicci and V. Kumar, "Robotic grasping and contact: A review," in *IEEE Int'l Conf. Robotics Automation*, April 2000.
- [16] R. Murray, Z. Li, and S. Sastry, *A Mathematical Introduction to Robotic Manipulation*. CRC Press, 1994.
- [17] R. Platt, "Learning and generalizing control-based grasping and manipulation skills," Ph.D. dissertation, University of Massachusetts, September 2006.
- [18] R. Platt, A. H. Fagg, and R. Grupen, "Extending fingertip grasping to whole body grasping," in *IEEE Int'l Conference on Robotics and Automation*, 2003.